

# Edge effects in compression testing periodic cellular metal sandwich cores

B. A. Bouwhuis · E. Bele · G. D. Hibbard

Received: 2 October 2007 / Accepted: 6 February 2008 / Published online: 11 March 2008  
© Springer Science+Business Media, LLC 2008

**Abstract** Compression testing of cellular sandwich core materials is often complicated by the presence of edge effects, in which the cells on the outside of the specimen deform at lower stresses than those in the bulk. As a result, minimum specimen length-to-cell-size ratios have been established in the literature for metallic foams. Periodic cellular metals (PCMs) are a recently developed class of materials that have received considerable interest due to their greater architectural efficiency and enhanced mechanical properties compared to conventional metal foams. In this study, edge effects of PCM core materials have been measured in compression using a new test platform which evaluates the properties of the core as a stand-alone material. This approach introduces uniform and periodically rigid boundary conditions to the PCM nodes, resulting in the same inelastic buckling failure mechanism that occurs in reference PCM sandwich panels. Edge effects were comparatively small and samples down to  $2 \times 2$  unit cells were found to be representative of bulk-like cores.

## Introduction

Periodic cellular metals (PCMs) have recently received considerable interest because of their greater architectural efficiency than conventional metallic foams, see recent

reviews [1, 2]. These are hybrid materials which are typically composed of columnar supports arranged to resolve an externally applied load axially along the members. In contrast, foams can have externally applied loads resolved transverse to the supporting members and deformation is thus bending dominated [1]. For a given columnar weight, the axial load to failure (e.g. buckling or yielding) is typically greater than the bending load to failure (e.g. plastic hinging or fracture); this generally results in PCMs having greater weight-specific properties than the conventional metal foams.

While cellular metals are often used as cores in sandwich panels, a key developmental step is their optimization as stand-alone materials. Overall, the properties of cellular metals are a function of the structural arrangement of the supporting material (i.e. architecture) as well as the internal metallurgical state (i.e. microstructure). The processing and manufacturing of PCMs is therefore guided by both architectural and microstructural considerations. Recently we have developed a test platform for studying the mechanical performance of stand-alone pyramidal PCM cores [3]; recessed steel channels in the compression platens (confinement plates) are used to lock the truss cores' nodes in place such that failure occurs by inelastic buckling, simulating the behaviour in a fully bonded sandwich panel. This platform has been successfully used as part of the development of hybrid nanocrystalline PCMs, where high-strength nanocrystalline sleeves were electroformed around a pyramidal aluminium alloy PCM pre-form [4]. Confinement plates were used to study the optimal trade-off in terms of weight penalty due to the nanocrystalline sleeves and the mechanical performance increase of the pyramidal truss core [4]. The initial part of this study builds on the initial work for pyramidal core PCMs [3] to look at the feasibility of using confinement plates for tetrahedral PCM cores.

---

B. A. Bouwhuis (✉) · E. Bele · G. D. Hibbard  
Department of Materials Science and Engineering,  
University of Toronto, 184 College Street, Toronto, ON,  
Canada M5S 3E4  
e-mail: bouwhui@ecf.utoronto.ca

G. D. Hibbard  
e-mail: glenn.hibbard@utoronto.ca

The second part of this study examines the significance of sample size in confined compression testing of PCMs. Sample size effects are a potentially significant complication in the mechanical testing of cellular sandwich core materials because the size of the cell structure is typically on the same scale as the sample itself. For example, there must be a minimum number of cells in metallic foam samples to reflect a statistical distribution of random imperfections [5]. In addition, fixing foams between face sheets (creating a sandwich panel) constrains the cells closest to the sheets, resulting in a through-thickness strain gradient during loading [6, 7]. Lastly, cells near the edges of the specimen are subjected to boundary-layer effects and constraint effects [8–12]; as a result, edge cells typically contribute less to the overall performance than cells in the middle of the specimen. To date, edge effects have not been systematically studied in PCM cores. The present study examines the mechanical testing of stand-alone tetrahedral PCM truss cores with a focus on the nature of edge effects present during compression testing.

## Experimental

Tetrahedral PCM truss cores were fabricated from a  $0.79 \pm 0.01$  mm thick ( $t$ ) hexagonal-punched aluminium

3003-H14 sheet, purchased from McNichols Perforated Products (Atlanta, GA). The  $34.92 \text{ mm}^2$  (internal edge length  $l_0 = 3.67$  mm) base metal perforations were arranged in a 2D hexagonal lattice, unit cell in Fig. 1a. The planar perforated structure is an array of 3-rayed nodes with strut cross-sections of  $0.79$  mm (width  $w$ )  $\times$  thickness  $t$ , having 79% open area. A modified perforation-stretching process, based on the method described by Sypeck and Wadley [13], was used to fabricate the PCM cores. Struts were stretched at room temperature by applying out-of-plane force at their intersections (nodes) using hardened steel dowel pins of  $1.1$  mm diameter. The forming load was applied using a Shimadzu screw-driven compression platform at a constant linear deformation rate ( $1$  mm/min) to achieve a PCM relative density (PCM density divided by AA3003 density) of 6.0% ( $0.16 \text{ g/cm}^3$ ). After fabrication, the mid-strut cross-section decreased from  $0.79 \times 0.79$  mm to  $0.76 \times 0.76$  mm. A schematic diagram of a PCM tetrahedral unit is shown in Fig. 1b.

A range of sample sizes were fabricated and are summarized in Table 1. Note that sample geometries were selected to contain only whole supporting members. Sample size was defined by the total number of ‘edge’ ( $n_T^{\text{edge}}$ ) and ‘bulk’ ( $n_T^{\text{bulk}}$ ) tetrahedral units, Table 1. Bulk tetrahedral units had three struts, with each strut intersecting adjacent struts at a three-rayed node. Edge units

**Fig. 1** Schematic diagrams of the perforated precursor dimensions prior to forming (a), a single PCM tetrahedron (b), and a sample of 33 tetrahedral units (sample S2 in Table 1) (c). The shaded region in (c) illustrates a 2-D hexagonal unit cell, while bulk and edge tetrahedral units are indicated by solid and dashed lines, respectively

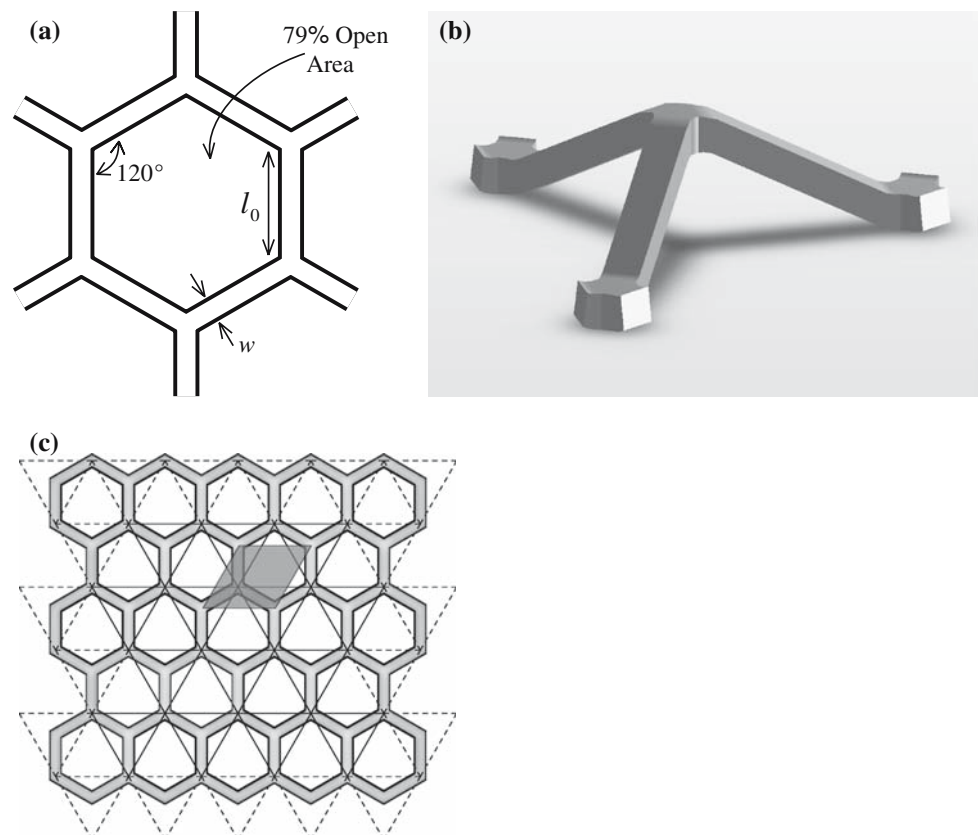


**Table 1** List of PCM truss core specimens tested and summary of architectural features: sample name (with number of repeats), total number of tetrahedra  $n_T$ , number of edge  $n_T^{edge}$  and bulk tetrahedra  $n_T^{bulk}$  (with fraction of total), and total number of struts  $n_S$

Name	$n_T$	$n_T^{edge}$	$n_T^{bulk}$	$n_S$
S1 (3)	52	25 (0.48)	27 (0.52)	142
S2 (3)	33	19 (0.58)	14 (0.42)	88
S3 (4)	15	11 (0.73)	4 (0.27)	38
S4 (6)	8	7 (0.88)	1 (0.12)	19
X (3)	29	28 (0.97)	1 (0.03)	71

had only two struts and/or two-rayed node connectivity. Figure 1c shows a schematic diagram of the S2 sample geometry having 19 edge and 14 bulk tetrahedral units. Of the 19 tetrahedral units making up the sample perimeter, 11 had only two struts, while 8 had three struts, but only two-rayed node connectivity. The total number of tetrahedra ranged from 8 to 52, while the fraction of bulk tetrahedra ranged from 0.03 to 0.52. The total number of struts per sample ranged from 19 to 142 (Table 1).

Uniaxial compression testing of PCM truss cores was performed at a cross-head displacement rate of 1 mm/min. Between three- and six-test trials were conducted for each sample size (Table 1); a greater number of trials were conducted for smaller test specimens, after [8]. Compressive strains were estimated from cross-head displacement [3, 9, 10, 14, 15]. The confined-core uniaxial compression mode was used to simulate truss core collapse in a sandwich panel. Single-layer tetrahedral PCM truss cores were fixed between confinement plates, which laterally confine

the nodes resulting in an inelastic buckling failure mechanism. The confinement plates were machined from AISI 1020 mild steel and had three sets of parallel recessed channels (0.8 mm deep) offset by 120° to confine the tetrahedral PCM truss core nodes, Fig. 2.

Reference sandwich structures were made by resistance brazing the tetrahedral truss cores to the same perforated sheet precursors used in forming. The joints were fabricated using molybdenum-capped electrodes of 1.6 mm tip diameter with a 66.7 N squeezing force, 0.17 s brazing time, and 80% of the maximum heat output from a UNITEK resistance welding machine (2.5 kVA power supply). The brazing paste, from Omni Technologies Corp. (Brentwood, NH), had an 80% KAIF<sub>4</sub>—15% K<sub>2</sub>AlF<sub>5</sub>—5% K<sub>3</sub>AlF<sub>6</sub> liquid flux and 88% Al—12% Si filler metal powder. Note that the diameter of the resistance welding electrodes (1.6 mm) was larger than the diameter of the steel dowel pin (1.1 mm) used for the perforation-stretching process. This flattened the truss nodes at the expense of strut length, see schematic diagrams in Fig. 3. The change in strut length was measured from cross-sections of the as-formed truss core and resistance-brazed sandwich panel; strut length decreased from 3.95 ± 0.15 mm in the as-formed PCM core to 3.48 ± 0.13 mm in the resistance-brazed sandwich panel. This change in strut length, accompanied by a negligible change in truss height  $h$  (2.72 ± 0.02 mm for the as-formed core and 2.71 ± 0.06 mm in the sandwich), meant that the truss angle  $\omega$  increased from 28.5 ± 0.1° in the as-formed core to 32.8 ± 0.1° in the resistance-brazed sandwich.

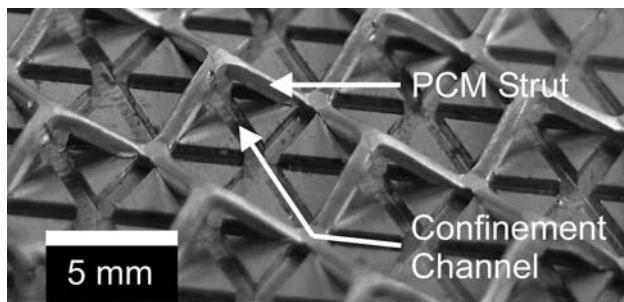


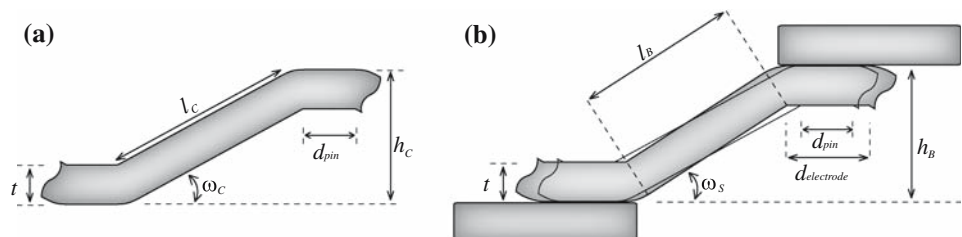
**Fig. 2** PCM truss core placed in the recessed channels of the bottom confinement plate used to simulate the nodal confinement in a sandwich panel

**Results and discussion**

**Simulating sandwich core collapse**

The force-displacement curve for uniaxial compression of the reference sandwich panel (with stress-strain axes also shown) is presented in Fig. 4. Post-compression analysis showed that all struts failed by an inelastic buckling mechanism and that none of the joints between truss core and facing sheet had failed. The same tetrahedral truss cores used to fabricate the reference sandwich panel were also compression tested using the confinement plates

**Fig. 3** Schematic cross-section of the as-formed truss core (a) and brazed sandwich panel (b) showing the truss angle  $\omega$ , truss height  $h$ , strut length  $l$ , thickness  $t$ , and pin/electrode diameter  $d$



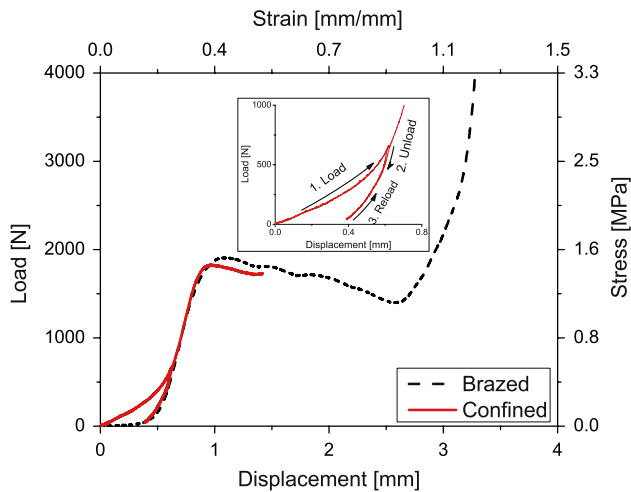


**Fig. 4** Load ( $F$ )–displacement ( $d$ ) and stress ( $\sigma$ )–strain ( $\epsilon$ ) curves of a confined-core PCM and a sandwich structure. Inset shows the load, unload, reload path used to fully seat the truss core in the confinement plate. Note that the strain was estimated from the cross-head displacement

shown in Fig. 2. Samples were loaded until the struts failed by inelastic buckling, i.e. until just after the initial peak force in the force–displacement curve ( $F_P$ ). A typical confined-core force–displacement curve is shown with the reference sandwich panel in Fig. 4. Note that truss cores tested in the confinement plates showed an initial bedding-in effect; however, once the truss core was fully seated in the confinement plate, e.g. by applying a small pre-load of  $0.33 F_P$  (see inset in Fig. 4), it exhibited nearly the same elastic force-displacement profile as the reference sandwich panel.

The relative peak strengths measured for the confined cores ( $1.88 \pm 0.04$  kN) and the reference sandwich panels ( $2.07 \pm 0.09$  kN), can be considered in terms of the changes in truss geometry caused by resistance brazing (Fig. 3). Recent PCM compression studies that have observed overall failure by inelastic buckling of supporting members (e.g. [2, 16, 17]) have modeled the inelastic response of the PCM struts after Engesser [18] and Shanley [19]. These studies investigated the axial load to invoke inelastic buckling,  $F_{\text{Inelastic}}$ , of a single ideal uniform column with tangent modulus  $E_T = \partial\sigma/\partial\epsilon$ :

$$F_{\text{Inelastic}} = \frac{k^2 \pi^2 E_T w t^3}{l^2 12} \quad (1)$$

where  $t$  and  $l$  are geometric parameters (Fig. 3),  $w$  is the strut width, and  $k$  is a constant reflecting the end constraints of the column. In practice, the inelastic buckling strength is reduced by fabrication defects and geometric imperfections [2, 17, 20]. This inelastic buckling force per strut can be incorporated into PCM analysis to give a predicted upper limit for the PCM peak force,  $F_P$ , measured during compression testing as:

$$F_P = \frac{n_S}{\sin \omega} F_{\text{Inelastic}} \quad (2)$$

Here,  $\omega$  is the truss angle and  $n_S$  is the total number of struts in the sample. Figure 3 illustrates that resistance brazing with a larger diameter electrode than the forming dowel pin had the effect of reducing the strut length,  $l$  and increasing the truss angle,  $\omega$  (i.e. effectively strengthening the sandwich panel). Collecting the changing geometric factors in Eqs. 1 and 2 gives the following ratio:

$$\frac{(F_P)_S}{(F_P)_C} = \left(\frac{l_C}{l_S}\right)^2 \frac{\sin \omega_C}{\sin \omega_S} \quad (3)$$

where subscripts  $S$  and  $C$  refer to the sandwich and confined-core structures, respectively. The observations of the present study agree well with the predictions of Eq. 3:  $(F_P)_S/(F_P)_C = 1.11 \pm 0.07$  and  $(l_C/l_S)^2 \cdot \sin \omega_C / \sin \omega_S = 1.14 \pm 0.09$ . While it is expected that there may be small differences in the end constraints for struts that have been brazed versus struts that have been locked in place by the confinement plates, the present results suggest that the measured difference in peak strength is largely determined by the changes in truss length and truss angle during the joining step.

The elastic properties of the reference sandwich and confined truss cores can be similarly compared. The loading stiffness  $S_L$  was taken as the maximum value of the tangent to the loading curve prior to  $F_P$ . The measured  $S_L$  values can be related to the axial stiffness of the PCM struts. Assuming all struts are axially compressed simultaneously under the applied force, the overall PCM stiffness per strut can be calculated using the work-energy method, e.g. [21]:

$$S_L = \frac{1}{\sin^2 \omega} \frac{E w t}{l} \quad (4)$$

where  $E$  is Young's modulus of the parent material. The geometrical factors controlling the stiffness can be collected from Eq. 4 to give:

$$\frac{(S_L)_S}{(S_L)_C} = \left(\frac{l_C}{l_S}\right) \frac{\sin^2 \omega_C}{\sin^2 \omega_S} \quad (5)$$

where  $(S_L)_S$  and  $(S_L)_C$  refer to the loading stiffness of sandwich and confined core trusses, respectively. Using the experimentally measured strut lengths and truss angles,  $\left(\frac{l_C}{l_S}\right) \frac{\sin^2 \omega_C}{\sin^2 \omega_S} = 1.03 \pm 0.12$ , which is consistent with the observation that there was no significant difference in the elastic region of the load-displacement curves of Fig. 4.

#### Edge effects in confined-core compression

The effect of sample size and fraction of edge tetrahedra was examined by compression testing a range of sample



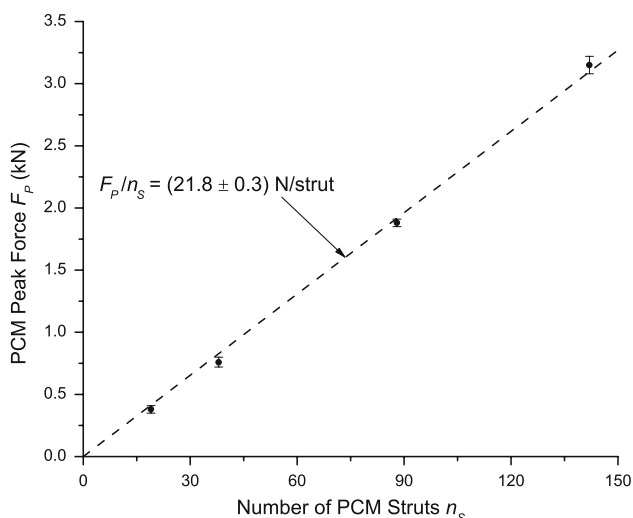


**Fig. 5** Measured PCM peak force,  $F_p$ , for the confined core samples as a function of the total number of PCM struts,  $n_s$

geometries all having the same truss core architecture. Samples were loaded until failure occurred by the same inelastic buckling mechanism as seen for the reference sandwich structure. The peak force values ranged from  $3.15 \pm 0.07$  N for sample S1 ( $n_s = 142$ ) to  $0.38 \pm 0.03$  kN for sample S4 ( $n_s = 19$ ). This is shown in Fig. 5 where the peak force  $F_p$  is plotted as a function of the total number of struts  $n_s$ ; a fitted linear relationship of  $F_p/n_s = 21.8 \pm 0.3$  N/strut is seen over the range from 19 to 142 total struts. Similarly, the maximum loading slope before the peak strength increased from  $0.81 \pm 0.14$  kN/mm for sample size S4 to  $7.73 \pm 0.56$  kN/mm for sample size S1 and can be seen in Fig. 6 giving a fitted linear relationship of  $S_L/n_s = 51.5 \pm 2.5$  N/mm·strut. Note that

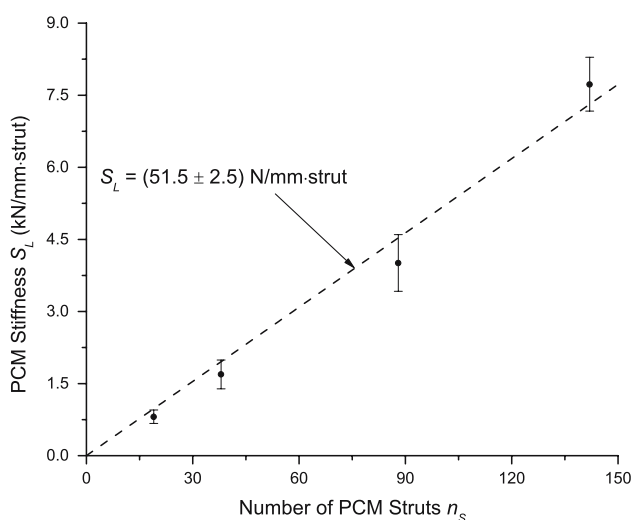


**Fig. 6** Measured PCM maximum loading stiffness,  $S_L$ , for the confined core samples as a function of the total number of PCM struts,  $n_s$

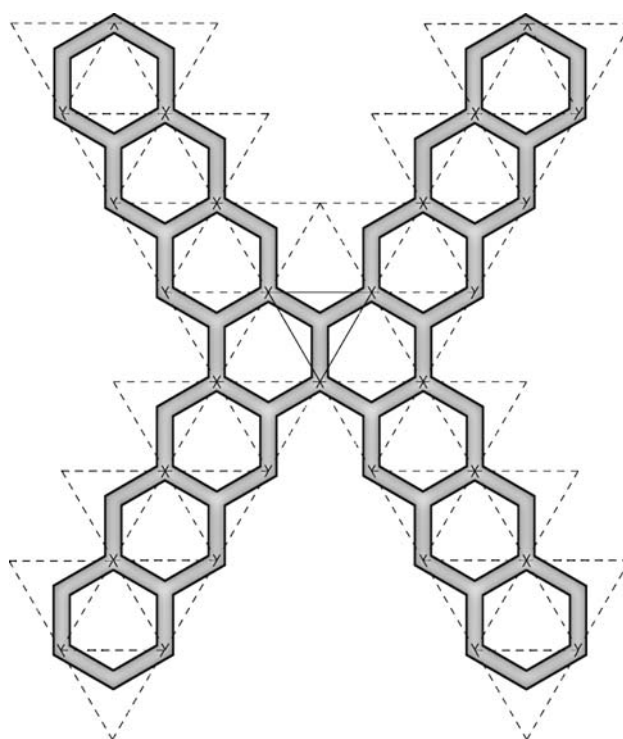


**Fig. 7** Schematic diagram of an X-shaped sample with high fraction (0.97) of edge tetrahedra (indicated by dashed lines)

these linear relationships occur despite the significant differences in the relative fractions of edge to bulk tetrahedra between the samples (Table 1). The relationships are also consistent with the prediction that edge effects become less significant as the regularity of the cellular architecture increases [9].

To investigate the significance of edge effects further, special X-shaped samples (Fig. 7) were fabricated. These samples had 71 total struts, of which 68 belonged to edge tetrahedral units. Of the 28 edge tetrahedral units making up the X-shaped sample perimeter, 16 had only two struts, while eight had three struts, but only two-rayed node connectivity. The measured peak strength and loading stiffness of the X-shaped coupon was  $1.40 \pm 0.01$  kN ( $19.7 \pm 2.0$  N/strut) and  $3.07 \pm 0.23$  kN/mm ( $43.3 \pm 3.3$  N/mm·strut); the peak is within one standard deviation, and the stiffness is within two standard deviations from the linear relationships shown in Figs. 5 and 6. This small effect of edge tetrahedra fraction is in significant contrast to conventional metallic foams where edge cells are less constrained and can cause a significant decrease in measured values. For example, Andrews et al. [10] studied edge effects in a closed-cell Alporas foam with an average cell size of 4.5 mm, as well as an open cell Duocel foam with cell size between 3.0 and 4.5 mm. In both cases, a 26% decrease in peak stress was found from larger samples (approximately  $8 \times 8$  cells in area) to small samples (approximately  $3 \times 3$  cells in area). Similarly for both

foams, a 20–29% decrease in unloading modulus was found for the same decrease in ratio of specimen size to cell size. The difference between foam edge effects and PCM edge effects may be understood more clearly through the analytical models of Onck et al. [11] for honeycomb materials: for whole (i.e. integer number) of cells comprising the specimens, the load-bearing capability is increased as the less capable cells (i.e. cut cells on the edges of the specimen) are not present. The ideal model of Onck et al. [11] predicts that for whole-cell specimens, the value of  $F_p/F_{p,Bulk}$  should remain equal to unity for specimen length-to-cell size ratios down to 1; this appears to agree well with the current results. In contrast, the ideal value of  $S_L/S_{L,Bulk}$  is expected to decrease to below 0.8 for specimen length-to-cell size ratios smaller than 3. The results of the present study show that the reduction in  $S_L$  is not as significant for PCMs as suggested for honeycombs by Onck et al. [11]. Due to the edge effects for conventional metallic foams, minimum ratios for the number of cells per sample dimension have been given in the range of 5–7 [9–12]. For PCMs, a similar (albeit smaller) minimum ratio can also be suggested where incomplete edge cells are included in the specimen [9].

Size effects can also be considered in terms of the sample-to-sample variability for a given test geometry. Figure 8 presents the standard deviation in the peak force measurements as a function of the number of total struts. The % variation in  $F_p$  (standard deviation divided by average  $F_p$ ) decreases from ~7% per strut for the smallest samples (S4, 19 struts) to below 3% for the larger samples (S1, 142 struts). For the limiting case of uniaxial compression testing of single columns, Perry and Chilver [22] found 5–10% variation for inelastic buckling failure, which is consistent with the increasing percent variation per strut

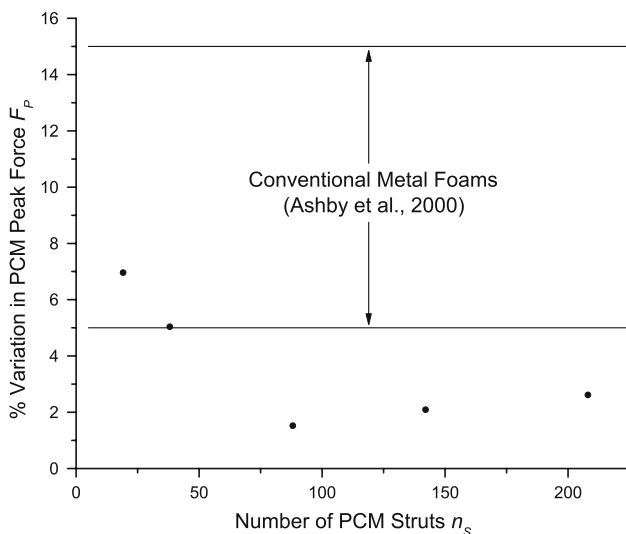


**Fig. 8** Percent variation in confined-compression peak force  $F_p$  (standard deviation divided by average  $F_p$ ) as a function of the total number of PCM struts within the specimens

with decreasing sample size found in the present study. Once buckling is initiated in the weakest member, the load is redistributed to the remaining supports which continue to buckle in a sequential fashion, e.g. [23–25]. On the other hand, the smaller percent variation for larger PCM samples is consistent with previous studies of conventional metallic foams, e.g. [10]. Furthermore, the % variation in  $S_L$  decreases from ~17% (S4) to ~7% (S1) with increasing specimen size. However, it should be noted that the percent variation measured for PCMs in the present study is lower than the values typically seen for foams; in the limit of testing a sufficiently large foam specimen to neglect size effects, the percent variation ranges from 5 to 15% for strength and 5 to 30% for stiffness [9–10]. It has been shown that as the number of cells in a cellular material increases, the statistical distribution of cell properties becomes more continuous, e.g. [26]. Further, the load capacity decreases quickly with the increasing percentage of failed cells [5]; therefore, the performance of samples with smaller numbers of cells will rely heavily on the performance distribution of single cells. Overall, as the dispersity of cell properties in a cellular material increases, its stability increases; this results in a decrease in deformation localization and a decrease in the scatter between test specimens [25].

The present results suggest that the confinement plates effectively provide the same *periodically rigid* boundary conditions throughout the sample. FEM models have been used to simulate this type of boundary condition as well as non-periodic conditions (e.g. rigid boundary conditions applied only to edge cells) and found that cell collapse occurs at a higher stress for the periodically rigid constraints, e.g. [5, 27]. The importance of periodic boundary conditions can also be seen from the mechanical test data of Zupan et al. [28], in which two confinement approaches were used. In the first, specimens were placed in a hollow box which restricted nodal spreading at the outer edge (i.e. rigid but non-periodic boundary conditions). In the second approach, nodes were bonded to face sheets using polyurethane adhesive providing a periodically rigid boundary condition. The non-periodic boundary conditions imposed by the hollow box resulted in plastic hinge-like deformation and a peak stress similar to the unconfined specimen (on steel platen interface). In contrast, the adhesively bonded specimen showed buckling-like deformation and a marked increase in both peak stress and stiffness, corresponding to a typical bulk PCM sandwich panel response. Overall, PCM cores can be tested in compression as stand-alone materials provided that the appropriate boundary conditions are applied to each truss core node. Furthermore, the confinement plates largely eliminate edge effects, allowing the PCM mechanical properties to be determined from relatively small-scale samples.

## Conclusions

This study developed a test method for evaluating the compressive performance of PCM truss cores. Edge effects, which are widely observed in conventional cellular foam materials, were examined in PCMs for stretching-dominated response (i.e. failure by inelastic buckling). Periodically rigid boundary conditions were applied uniformly to each node of the PCM truss core using confinement plates, which simulates the behaviour in a sandwich panel. This test method determines the buckling strength on a per-strut basis. No significant edge effects are seen over an order of magnitude range in strut number. It was found that meaningful compression data can be obtained from truss cores with specimens as small as  $2 \times 2$  unit cells.

**Acknowledgements** The authors would like to acknowledge the National Science and Engineering Research Council of Canada (NSERC) for funding. One of the authors, B.A.B. is also supported by an Ontario Graduate Scholarship for Science and Technology (OGSST).

## References

- Ashby MF (2005) *Philos Mag* 85:3235
- Wadley HNG (2006) *Philos Trans R Soc Lond A* 364:31
- Bouwhuis BA, Hibbard GD (2006) *Metall Mater Trans B* 37:919
- Suralvo M et al (2008) *Scripta Mater* 58:247
- Chen C et al (1999) *J Mech Phys Solids* 47:2235
- Bastawros A-F et al (2000) *J Mech Phys Solids* 48:301
- Chen C, Fleck NA (2002) *J Mech Phys Solids* 50:955
- Brezny R, Green DJ (1990) *J Mater Sci* 25:4571
- Ashby MF et al (2000) *Metal foams – a design guide*. Butterworth-Heinemann, Boston, pp 26–72
- Andrews EW et al (2001) *Int J Mech Sci* 43:701
- Onck PR (2001) *Int J Mech Sci* 43:681
- Onck PR (2003) *MRS Bull April*:279
- Sypeck DJ, Wadley HNG (2002) *Adv Eng Mater* 4:759
- Simone AE, Gibson LJ (1998) *Acta Mater* 46:3109
- Ramamurty U, Paul A (2004) *Acta Mater* 52:869
- Deshpande VS, Fleck NA (2001) *Int J Solids Struct* 38:6275
- Kooistra GW et al (2004) *Acta Mater* 52:4229
- Engesser F (1889) *Zeitschrift des Architekten und Ingenieur – Vereins zu Hannover* 35:455
- Shanley FR (1947) *J Aeronaut Sci* 14:261
- Wadley HNG et al (2003) *Compos Sci Technol* 63:2331
- Beer HNG, Johnston ER (1992) *Mechanics of materials*, 2nd edn. McGraw-Hill, Toronto, pp 570–600
- Perry SH, Chilver AH (1976) *Proc Inst Civ Eng Part 2 – Res Theory* 61:109
- Schmidt LC et al (1982) *J Struct Div* 108:1324
- Hanaor A et al (1989) *J Struct Eng* 115:1021
- Schraad MW (2007) *Mech Mater* 39:183
- Tekoglu C, Onck PR (2005) *J Mater Sci* 40:5911
- Öchsner A, Lamprecht K (2003) *Mech Res Comm* 30:573
- Zupan M et al (2003) *Int J Mech Sci* 45:851